



JOURNAL OF
APPLIED
CRYSTALLOGRAPHY

Volume 52 (2019)

Supporting information for article:

Air heated solid-gas reaction setup for *in situ* neutron powder diffraction

Jakob Voldum Ahlburg, Emmanuel Canévet and Mogens Christensen

Supporting information for:

Air heated solid-gas reaction setup for *in situ* neutron powder diffraction .

Jakob Voldum Ahlburg,^a Emmanuel Canévet,^{b,c} Mogens Christensen.^a

a. Center for Materials Crystallography, Department of Chemistry and iNANO, Aarhus University, Langelandsgade 140, 8000 Aarhus, Denmark

b. Laboratory for Neutron Scattering and Imaging, Paul Scherrer Institut (PSI), 5232 Villigen, Switzerland

c. Department of Physics, Technical University of Denmark, 2800 Kgs. Lyngby, Denmark

The supporting information includes the refined parameters for the *in situ* reduction of CoFe_2O_4 .

Model:

The sequential refinement carried out was done in two parts. In the first four patterns the model only contains CoFe_2O_4 crystallographic and magnetic phase. It is based on the refinement seen in Figure 4 **a**). The phase was described in the space group $Fd\bar{3}m$ using the atomic positions in Tabel S1. The tetrahedral and the octahedral sites are both partially occupied by Co^{2+} and Fe^{3+} .

| $Fd\bar{3}m$ | x | y | z |
|------------------|---------|---------|---------|
| Oxygen | 0.25432 | 0.25432 | 0.25432 |
| Tetrahedral site | 0.125 | 0.125 | 0.125 |
| Octahedral site | 0.5 | 0.5 | 0.5 |

Table S1: atomic positions for the $Fd\bar{3}m$ CoFe_2O_4 .

The refined parameters in this case were background, scale factor, unit cell parameters, Lorentzian isotropic peak broadening (γ), isotropic thermal vibration (B_{overall}), site occupation (tetrahedral and octahedral) and average magnetic moment of the octahedral and tetrahedral site.

From pattern 5 to 39 the model furthermore includes a crystallographic phase for $\text{Co}_{.33}\text{Fe}_{.67}\text{O}$ and a crystallographic and magnetic phase for CoFe_2 .

The $\text{Co}_{.33}\text{Fe}_{.67}\text{O}$ is described with the space group $Fm\bar{3}m$ using the atomic positions in Tabel S2. The refined parameters for the phase are scale factor, unit cell parameters and Lorentzian isotropic peak broadening (γ). It was not possible to refine the B_{overall} and it was fixed at $B_{\text{overall}} = 1.4$.

| $Fm\bar{3}m$ | x | y | z |
|--------------|-----|-----|-----|
| Oxygen | 0.5 | 0.5 | 0.5 |
| Metal | 0 | 0 | 0 |

Table S2: Atomic position for the $Fm\bar{3}m$ $\text{Co}_{.33}\text{Fe}_{.67}\text{O}$.

The CoFe_2 is described with the space group $Pm\bar{3}m$ using the atomic positions in Table S3. The metal 1 site is occupied fully by Fe and the metal 2 site is occupied with a ratio of Co:Fe of 2:1. The refined parameters for the phase are scale factor, unit cell parameters and Lorentzian isotropic peak broadening (γ). It was not possible to refine the B_{overall} and it was fixed at $B_{\text{overall}} = 1.94$. It was not possible to refine the magnetic moment and it was fixed at $3.466 \mu_B$ which was achieved from the final refinement in Figure 4 **b**).

| $Pm\bar{3}m$ | x | y | z |
|--------------|-----|-----|-----|
| Metal 1 | 0 | 0 | 0 |
| Metal 2 | 0.5 | 0.5 | 0.5 |

Table S3: Atomic positions for the $Pm\bar{3}m$ $CoFe_2$

Results:

The refined average magnetic moment of the $CoFe_2O_4$ phase is presented in Figure S1. The general trend shows a slight increase during the experiment but as with the unit cell parameter for the phase presented in Figure 6 **b**) it has an abrupt value at $t = 8$ min. The general increase can be described as a spring-exchange with the pure $CoFe_2$ that grows stronger with the amount of $CoFe_2$ in the sample. The size of the uncertainties comes from the lack of peaks present in the data achievable at the DMC beamline, which has a limited Q-range.

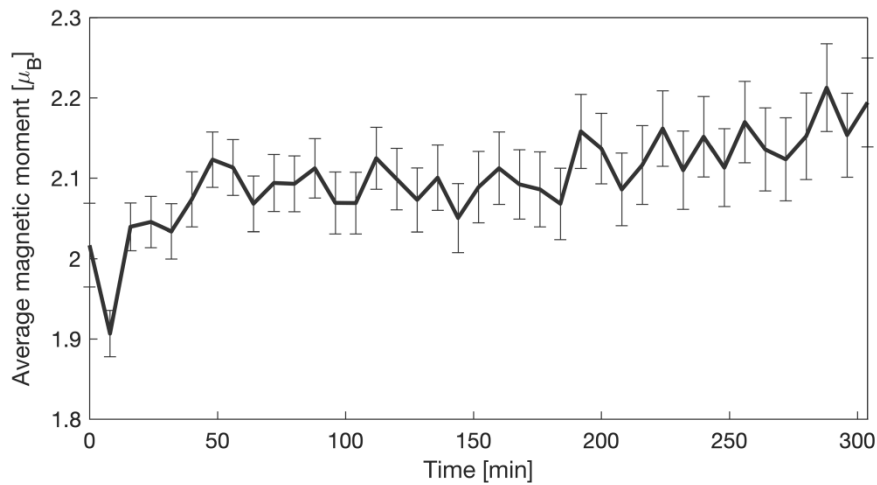


Figure S1: Refined average magnetic moment of the $CoFe_2O_4$ phase as a function of time.

In Figure S2 the R_f factors for all three phases are presented. All values are below 10% and there are no sudden jumps in the curves which indicates no sudden changes or discrepancies in the description of the structure factors.

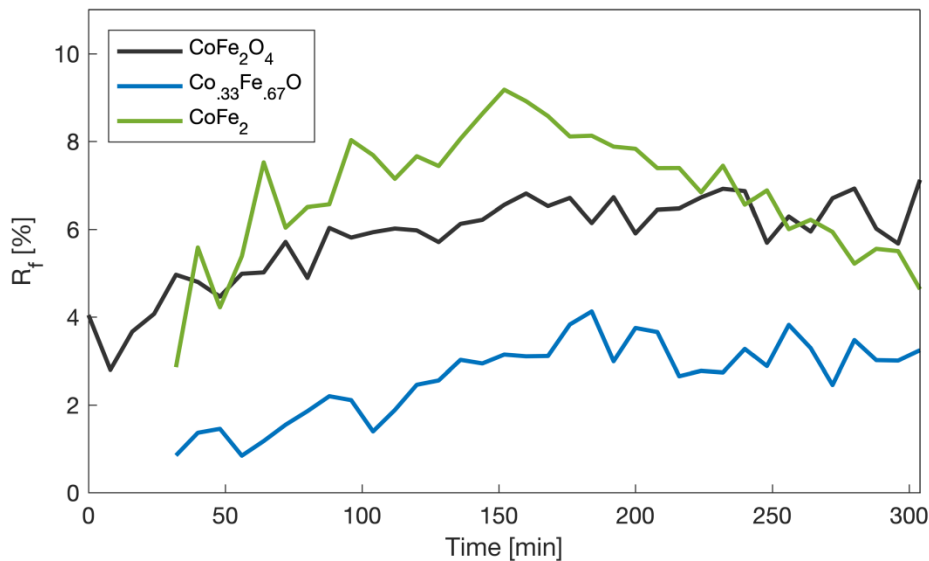


Figure S2: R_f factors for the three phases as a function of time

Figure S3 shows the weighted profile R -factor R_{wp} and the χ^2 . Both curves are almost constant except for the first pattern where both values are significantly higher. This is due to the heating of the sample which happens during the first pattern. The R_{wp} values are $\sim 21\%$, which is somewhat higher than you would normally expect. This can be explained in multiple ways; either the powder statistics are not high enough during the experiment or it is the low background which gives the uncertainty on the intensities a higher weighting as discussed by McCusker, L. B. *et al.* (1999) and Toby, B. H. (2006) Since the background during most of the experiment is very low and all other refined parameters show reasonable uncertainties most of the reason for the high R_{wp} lies with the low background. Finally the χ^2 has a value of ~ 2.5 during most of the experiment. This shows that R_{wp} is close to the expected R factor R_{exp} and that the model fits the data well.

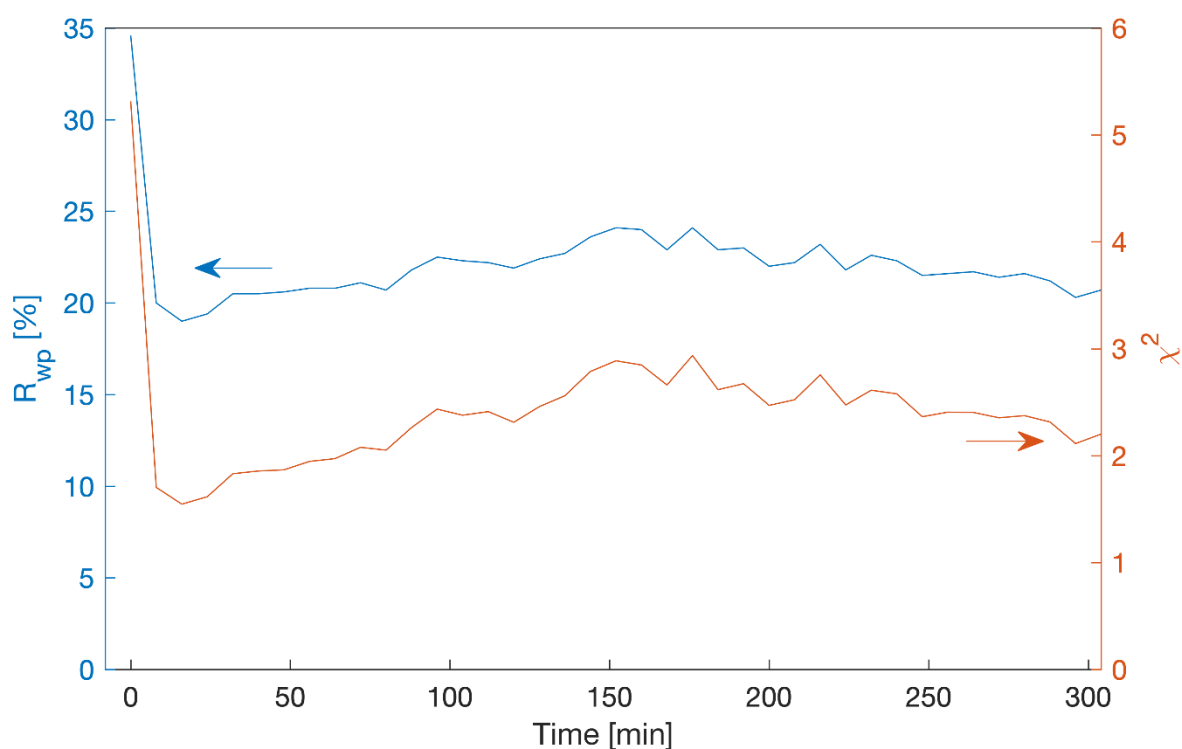


Figure S3: R_{wp} and χ^2 as a function of time

References

- McCusker, L. B., Von Dreele, R. B., Cox, D. E., Louer, D. & Scardi, P. (1999). *J Appl Crystallogr* **32**, 36-50.
Toby, B. H. (2006). *Powder Diffraction* **21**, 67-70.